Supplementary Figures S1-S9

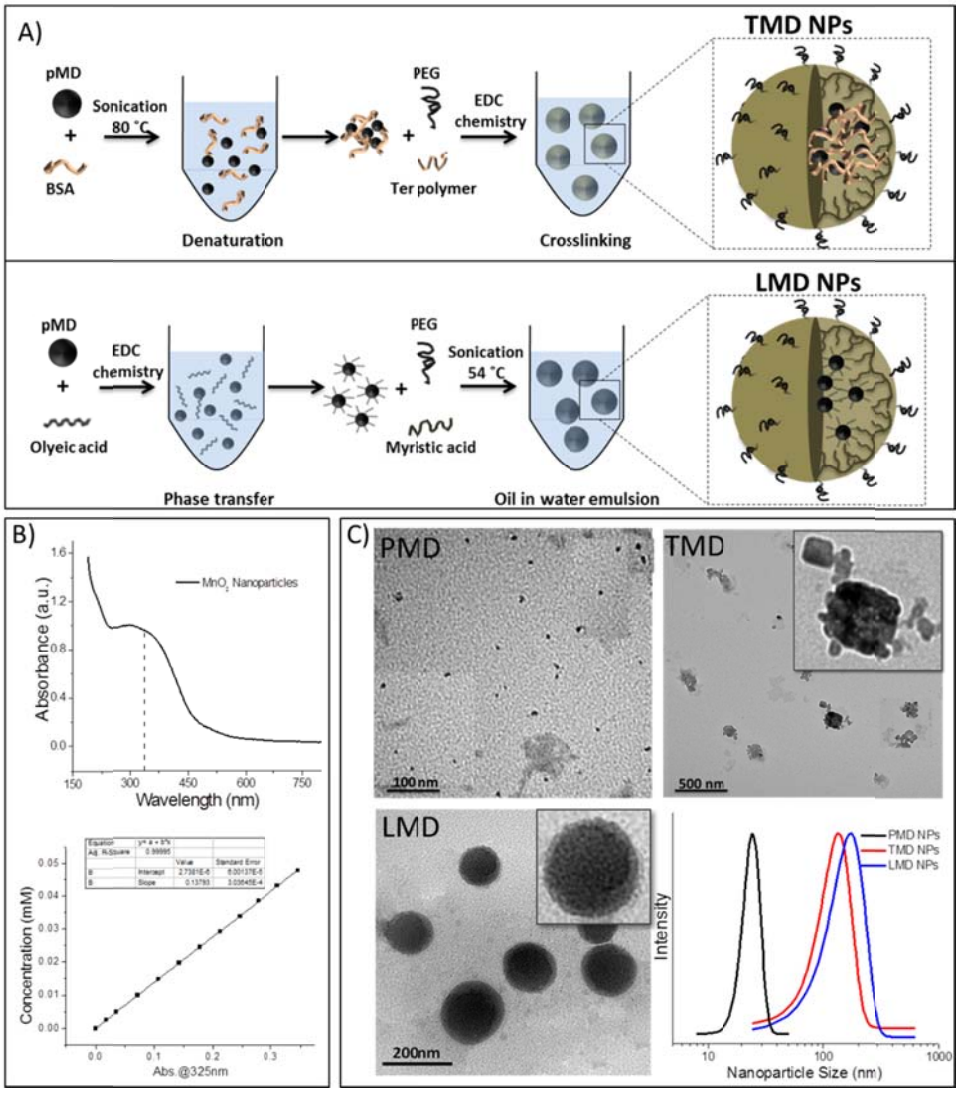

Fig. S1: Characterization of NPs. A) Schematic diagrams of TMD and LMD and their synthesis procedure;. B) Absorbance spectrum of precursor MD NPs (PMD), and calibration curve obtained by plotting the absorbance at 325 nm versus concentration of Mn obtained from ICP-AES analysis. The calibration curve was used throughout the study to obtain the MD NPs concentration. C) Transmission electron microscope image of PMD, TMD and LMD NPs and the size distribution obtained using Zetasizer.

Figure S2. Immunofluorescence detection of tumor hypoxia following intratumoral (IT) treatment of MDNPs

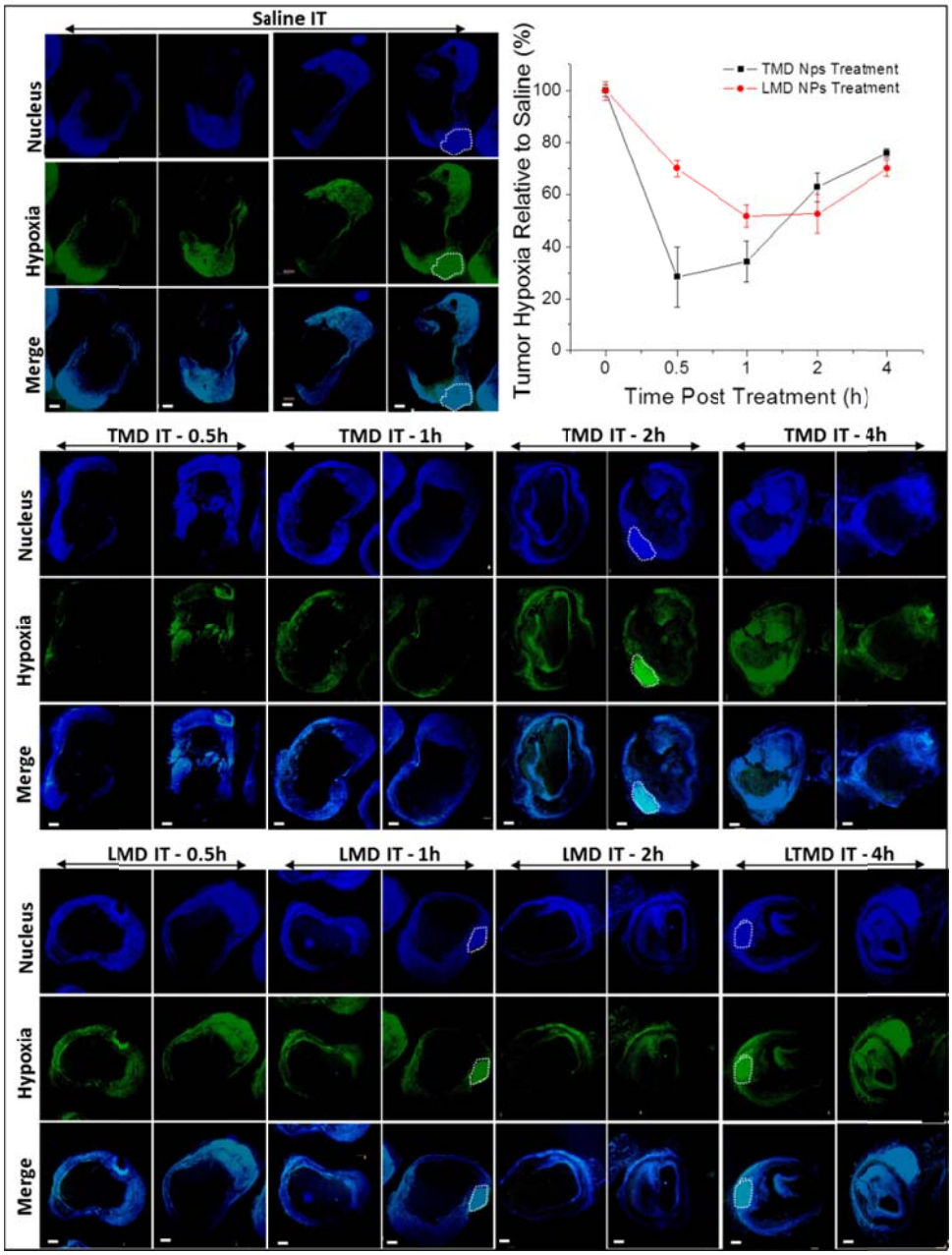

Fig. S2: Immunofluorescence (IF) detection and quantification of EMT6 tumor hypoxia. Panels shows representative IF images of whole tumor tissues treated with saline, TMD or LMD NPs (50 μL, 1 mM MnO_2) by local IT after various time points post injection up to 4 h. Detection of tumor hypoxia was determined by pimonidazole binding (green) using Hypoxyprobe-1 plus kit. Nuclei (blue) were stained with DAPI. The lymph nodes in tumors are indicated with dotted line. These areas and necrotic regions were excluded from quantitative image analysis. In all images scale bar correspond to 1 mm.

Figure S3. Immunofluorescence detection of tumor hypoxia following intravenous (IV) treatment of MDNPs

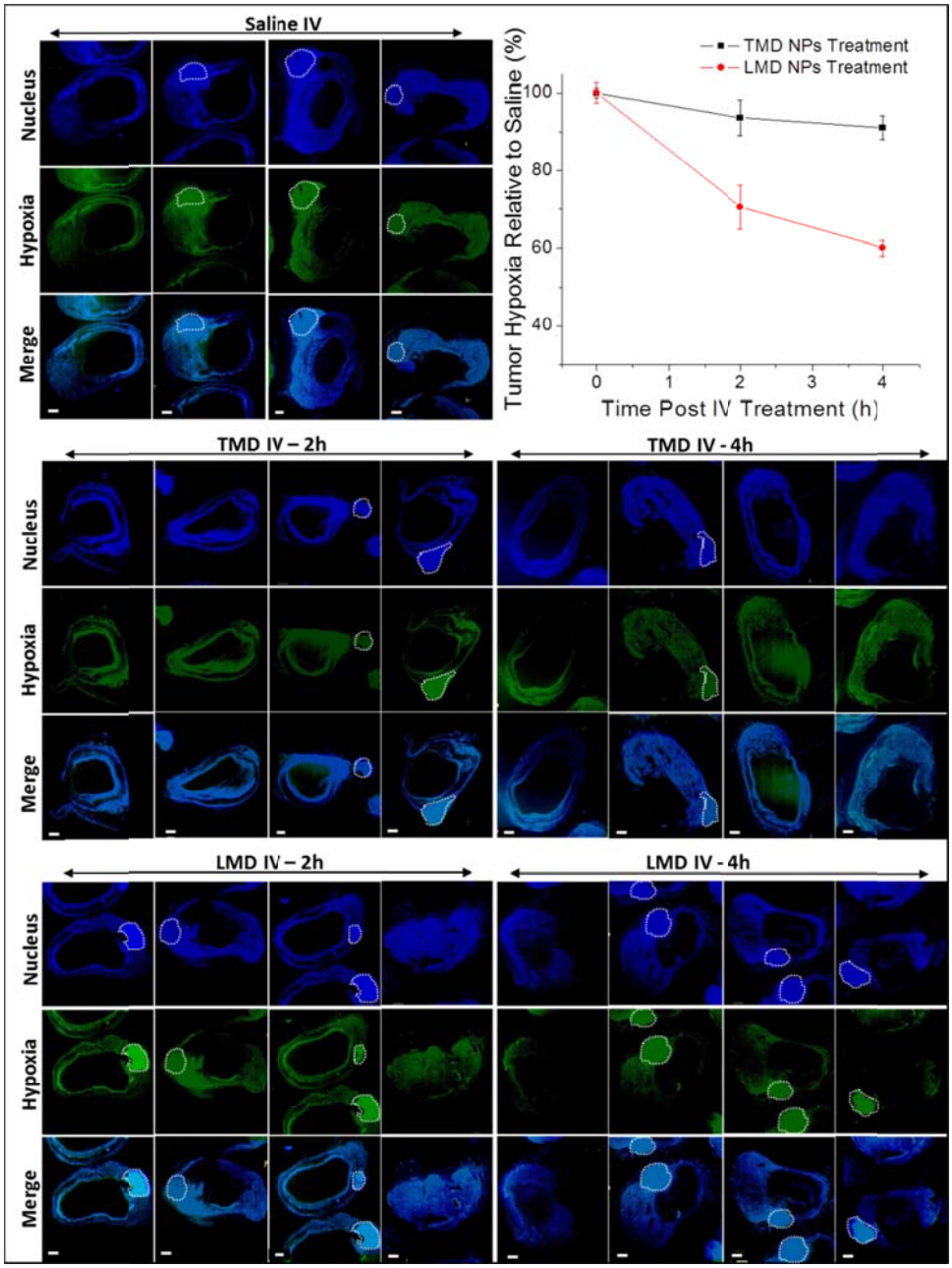

Fig. S3: IF detection and quantification of EMT6 tumor hypoxia. Panel shows representative IF images of whole tumors tissues treated with saline, TMD and LMD NPs (50 µL, 1 mM MnO_2) through systemic IV injection after various time points post injection up to 4 h. Detection of tumor hypoxia was determined by pimonidazole binding (green) using Hypoxyprobe-1 plus kit. Nuclei (blue) were stained with DAPI. The lymph nodes in tumors are indicated with dotted line. These areas and necrotic regions were excluded from quantitative image analysis. In all images scale bar correspond to 1 mm.

Figure S4

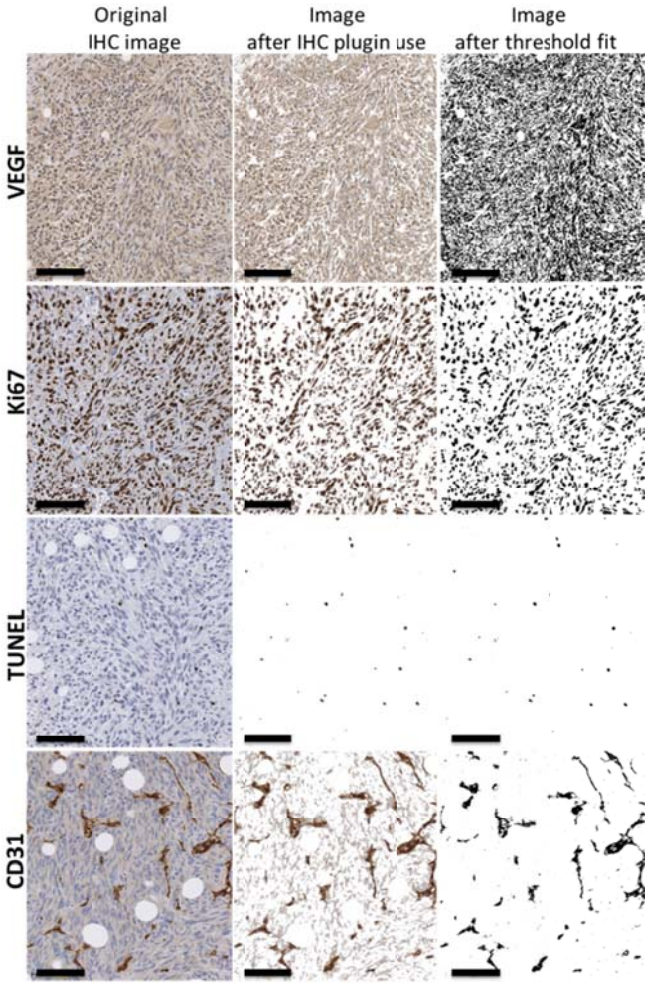

Figure S4. Quantification of IHC images. This figure shows an example of the image analysis of IHC data. Left column "Original IHC image" represents the original DAB staining of VEGF, Ki67, TUNEL and CD31, respectively. IHC plugin of ImageJ program was used to select the positive color pixels in DAB stained images and to eliminate the background color pixels resulting in "Image after IHC plugin Use" (middle column). The threshold plugin was then used to carefully select the positive stained area and minimize the background signal "Image after threshold fit" (right column). Finally the percentage of stained area was measured and plotted for each treatment group. In the case of apoptosis, positive TUNEL stained nuclei were counted for each IHC image and the length and the width of the field were used to calculate the positive nuclei per mm^2. Scale bar correspond to 100 μm.

Figure S5

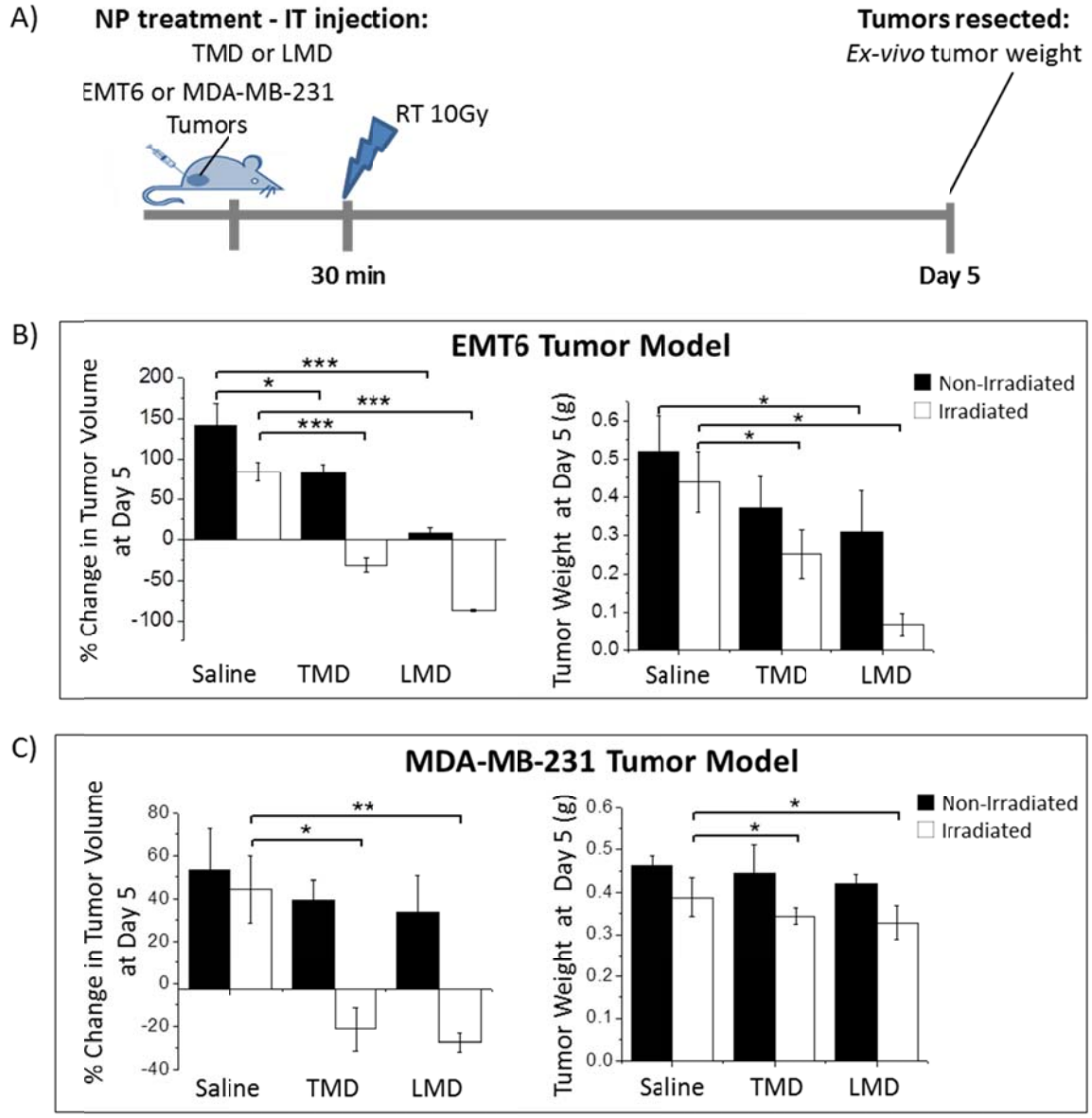

Figure S5. Effect of IT treatment with MDNPs alone or combined with RT on murine and human breast tumors growth. Tumors received IT treatment with saline+/-RT, TMD+/-RT, and LMD+/-RT. A) A schematic diagram showing the experimental design. Percentage change in tumor volume (right panel) and in *ex vivo* tumor weight (left panel) at day 5 post-treatments in EMT6 tumor model (B) and in MDA-MB-231 tumor model (C). Data are presented as mean ± SD (n = 3). (*) Statistically significant difference (*P < 0.05, **P < 0.01 and ***P < 0.001 when compared to respective saline group).

Figure S6

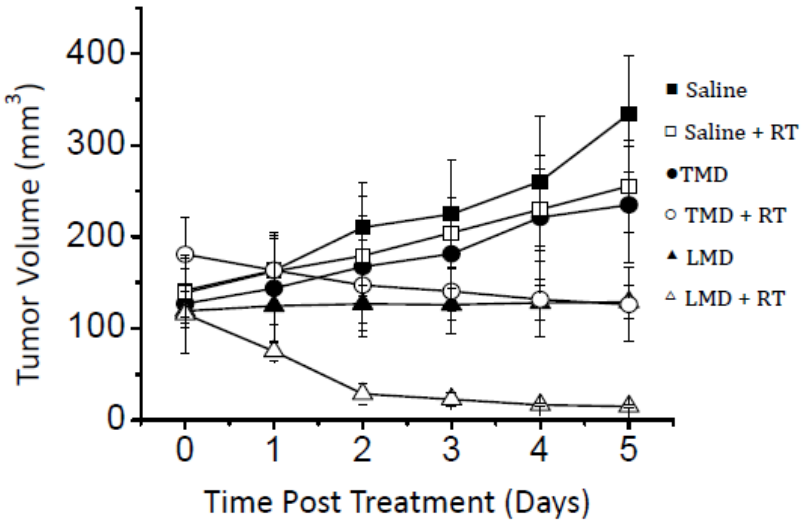

Figure S6. Effect of IT administered MDNPs alone or in combination with RT on the growth of murine EMT6 breast tumor. Tumors were treated IT with saline+/-RT, TMD+/-RT, and LMD+/-RT. For RT groups, irradiation was applied 30 min post injection of the various formulations or saline. The tumor volume was measured daily for up to 5 days. Data are presented as mean ± SD (n = 5/group).

Figure S7

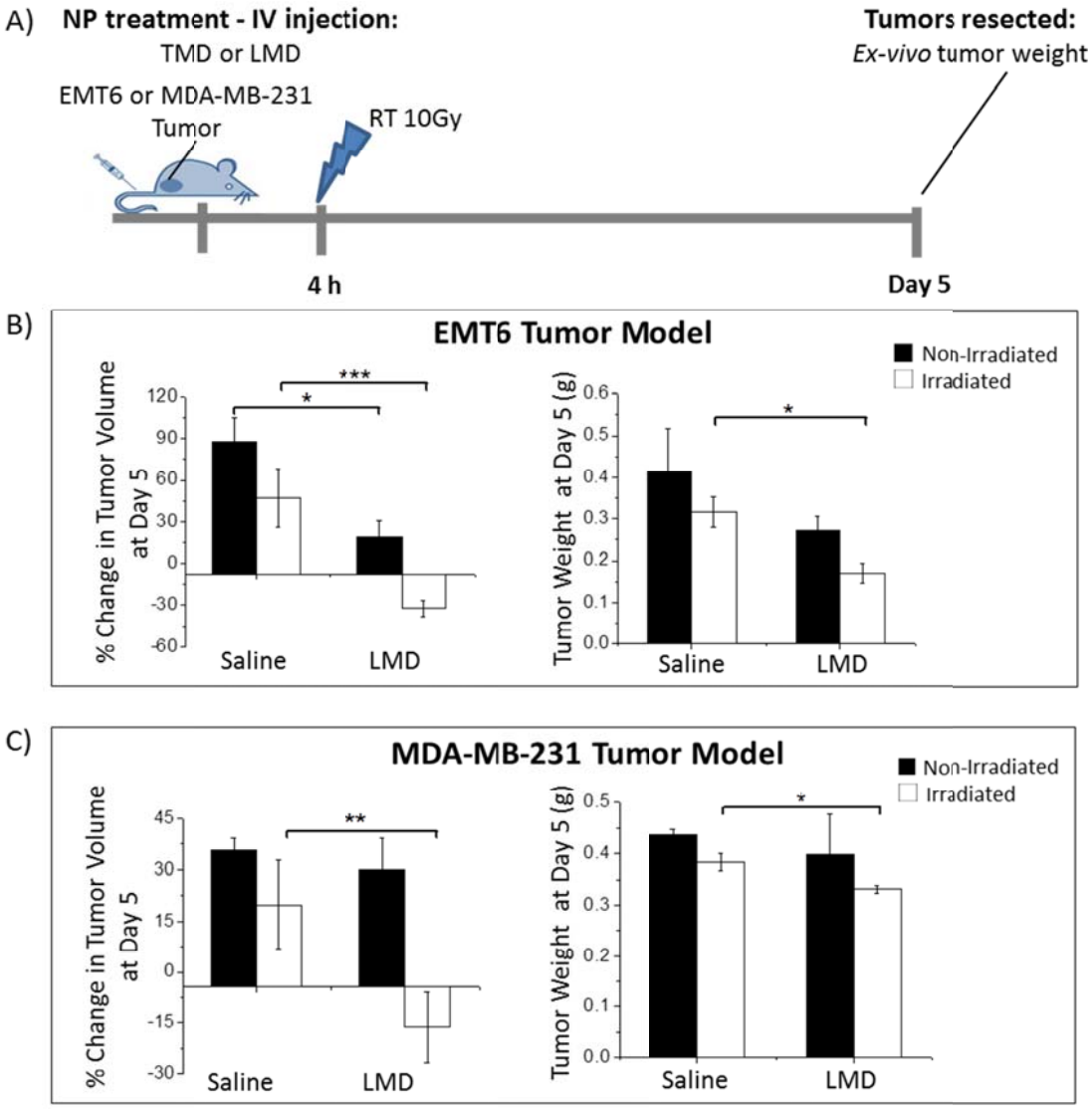

Figure S7. Effect of IV treatment with MDNPs alone or combined with RT on murine and human breast tumors growth. Tumors were treated IV with saline+/-RT, LMD+/-RT. A) A schematic diagram of the experimental design. Percentage changes in tumor volume (left panel) and in *ex vivo* tumor weight (right panel) at day 5 in EMT6 tumor model (B) and in MDA-MB-231 tumor model (C). Data are presented as mean ± SD (n = 3). (*) Statistically significant difference (*P < 0.05, **P < 0.01 and ***P < 0.001 when compared to respective saline group).

Figure S8

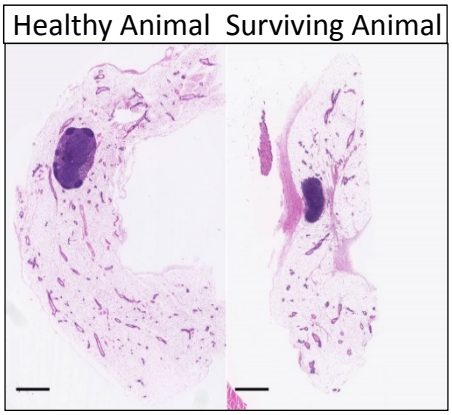

Figure S8. H&E stained mammary fat pad tissues of a healthy mouse and a LMD+RT surviving mouse. The mammary fat pad tissue of LMD+RT surviving animal was resected at 120 days post-treatment. Scale bars correspond to 100 μm.

Figure S9

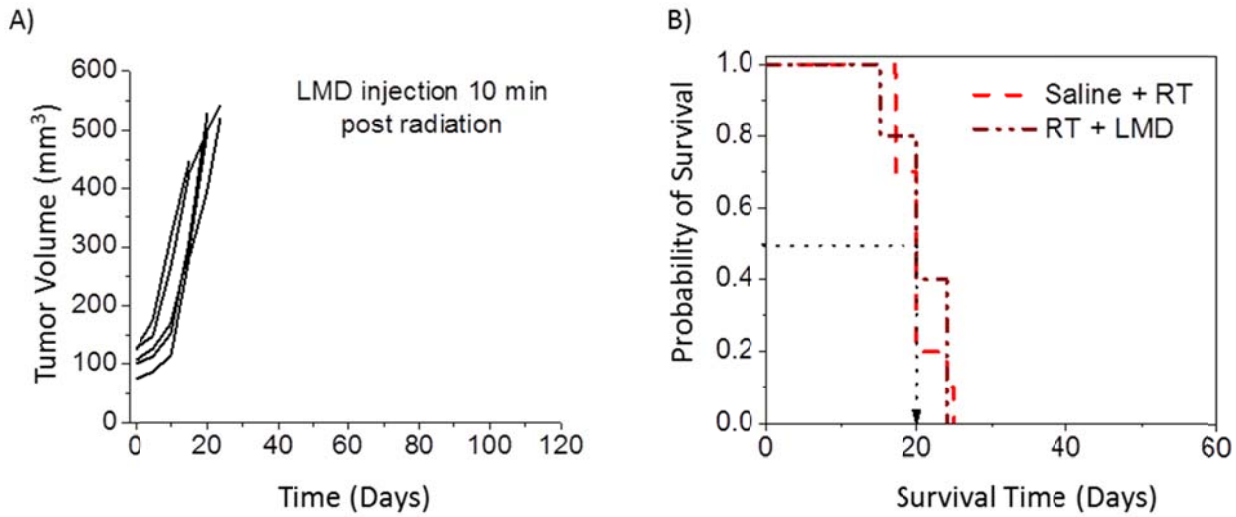

Figure S9. Effect of MDNPs treatment post irradiation. To eliminate the possibility that the enhancement of RT efficacy by MDNP is due to mechanisms other than oxygenation prior to irradiation, LMD NPs was injected IV 10 min post RT. A) Long term survival curves for animals treated IV with LMD NPs (200 μL, 1 mM MnO_2) 10 min post RT (n =5/group). Each curve represents one animal. B) Corresponding Kaplan Meier survival curve. For comparison Kaplan Meier survival curve for Saline + RT group is also added in the plot. The median survival time of both treatment groups overlap (20 days for both groups). This result is consistent with the hypothesis that the ability of LMD NPs + RT to extend the survival time of mice is due to the oxygenation of tumor microenvironment by LMD NPs when given an appropriate time before radiation. Horizontal dotted line is 50% survival level.